European Journal of Pharmaceutics and Biopharmaceutics 74 (2010) 120–125

Contents lists available at ScienceDirect

European Journal of Pharmaceutics and Biopharmaceutics

journal homepage: www.elsevier.com/locate/ejpb

Research paper

Non-invasive MRI detection of individual pellets in the human stomach

Manfred Knörgen [a], Rolf Peter Spielmann [a], Ahmed Abdalla [b], Hendrik Metz [b], Karsten Mäder [b,*]

[a] Department of Diagnostic Radiology, Martin-Luther-University of Halle, Halle, Germany
[b] Institute of Pharmacy, Martin-Luther-University of Halle, Halle, Germany

ARTICLE INFO

Article history:
Received 27 April 2009
Accepted in revised form 30 September 2009
Available online 12 October 2009

Keywords:
MRI
NMR-imaging
Pellets
In vivo
Stomach
Oral drug delivery
Multi-particulates
Magnetite

ABSTRACT

MRI is a powerful and non-invasive method to follow the fate of oral drug delivery systems in humans. Until now, most MRI studies focused on monolithic dosage forms (tablets and capsules). Small-sized multi-particulate drug delivery systems are very difficult to detect due to the poor differentiation between the delivery system and the food. A new approach was developed to overcome the described difficulties and permit the selective imaging of small multi-particulate dosage forms within the stomach. We took advantage of the different sensitivities to susceptibility artefacts of T_2-weighted spin-echo sequences and T_2-weighted gradient echo pulse sequences. Using a combination of both methods within a breath hold followed by a specific mathematical image analysis involving co-registration, motion correction, voxel-by-voxel comparison of the maps from different pulse sequences and graphic 2D-/3D-presentation, we were able to obtain pictures with a high sensitivity due to susceptibility effects caused by a 1% magnetite load. By means of the new imaging sequence, single pellets as small as 1 mm can be detected with high selectivity within surrounding heterogeneous food in the human stomach. The developed method greatly expands the use of MRI to study the fate of oral multi-particulate drug delivery systems and their food dependency in men.

1. Introduction

The peroral administration of drugs is the most frequently used route. An effective and safe therapy is based on reproducible and reliable pharmacokinetics. In many cases, a controlled release of the drug is desirable to avoid peak concentrations and decrease the frequency of the application. However, during the last years, it has been recognized that a high variability of the time course and the overall amount of drug absorption arises from the uncertainty of the stomach residence time of the dosage form. The time range of the emptying of tablets from the stomach into the small intestine might be in the range of a few minutes, but it might also exceed 10 h [1]. It is known that the size of the dosage form and the presence of food are the key parameters for the stomach emptying time. A very high variability of the stomach residence time of larger single dosage forms has been found. Therefore, multi-particulate dosage forms (pellets, mini-tablets, granules, see Fig. 1) with controlled release characteristics are replacing larger single-unit-controlled release tablets. The reasons are the decreased food dependency of gastric emptying and the higher predictability (advantage of the statistics of many particles vs. one particle). Although the general advantage of multi-particulate dosage forms are well accepted, many important questions remain to be answered. Examples include:

(1) How do the dosage forms distribute in the stomach in dependency from the kind and amount of food and the intake time?
(2) What is the impact of food induced changes of the shear forces on the release properties?
(3) How do multi-particulates designed for gastro-retention really stay in the stomach?

It is often claimed that pellets leave the stomach without food dependency and with a low variability; however, a recent study suggested that gastric motility contributes to a significant amount to the emptying of pellets. Considerable variability and also lag times of pellets emptying have been observed [2]. However, a non-direct pharmacokinetic approach has been used for this study, and the percentage of pellets which remained in the stomach was calculated but not measured. It is, therefore, important to develop and improve methods which are capable to visualize multi-particulate dosage forms in vivo in humans. It would be desirable, if a non-invasive, nonradioactive method could be used which could also track the stomach emptying and the distribution of food.

Gamma scintigraphy is still the main method to monitor dosage forms in humans and animals [3,4]. However, alternative methods

* Corresponding author. Institute of Pharmaceutics and Biopharmaceutics, Martin-Luther-University of Halle, Wolfgang-Langenbeck-Str. 4, D-06120 Halle (Saale), Germany. Tel.: +49 345 55 25167; fax: +49 345 55 27029.
E-mail address: Karsten.Maeder@pharmazie.uni-halle.de (K. Mäder).

0939-6411/$ - see front matter © 2009 Elsevier B.V. All rights reserved.
doi:10.1016/j.ejpb.2009.09.013

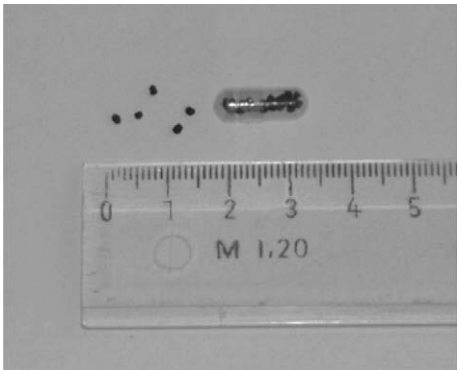

Fig. 1. Photograph of 1% magnetite-loaded pellets.

like magnetic resonance imaging (MRI, MRT) [5], magnetic marker monitoring (MMM) [6,7], biosusceptometry [8] and ESR [9,10] have attracted increased attention during the last years. Especially, MRI has a high potential to compete with gamma scintigraphy. The main advantages of this method are the avoidance of ionization radiation, the big scan volume and the easy combination with anatomical MR-images. However, some drawbacks should be mentioned: An MRI-inherent limit is the poor SNR, which can be raised (at a given hardware) only for longer measurement times. Yet an extension of the measurement time causes additional problems, which arises from physiological boundaries. Normally, the breath holding time of a healthy volunteer seldom exceeds 30 s. A much stronger limitation arises from the stomach contractions, whereby the mean duration of one stomach contraction cycle is approximately 18 s [11]. Typical pulse sequences on modern MRI scanners take 1 s per slice, leading to measurement times of ca. 20 s for the whole stomach.

In vivo MRI contrast enhancement can be achieved by the labelling of the drug delivery system with (super-)paramagnetic agents like Fe_3O_4 (magnetite) or gadolinium chelates (Gd-DOTA). Due to the strong susceptibility artefacts of Fe_3O_4-labelled pellets, tablets, capsules or other formulations, a visualization of the local drug distribution, its motion in the gastrointestinal tract and its decomposition is principally possible [12,13]. Also, the high availability, safety and non-problematic applicability for in vivo experiments are good reasons for the use of iron oxide-marked drugs for localization measurements by MRI. However, the application of this method has been restricted to the monitoring of strong susceptibility effects of large dosages until now [5], whereas smaller sized multi-particulate drug delivery systems (pellets, mini-tablets or granules) are very difficult to detect within a heterogeneously filled stomach. The reasons are the small size of the multi-particulate drug delivery systems and the poor selectivity of susceptibility artefacts. Although many pulse sequences show a good sensitivity, it is often difficult to differentiate between artefacts arising from surface effects of normal tissue boundaries, air bubbles or food heterogeneities and susceptibility effects of smaller super-paramagnetic labelled drug forms. With respect to the broad use and increasing importance of multi-particulate drug delivery systems, it was, therefore, the aim of the current study to develop new experimental setups which permit the detection of oral multi-particulate delivery systems and their discrimination from food and air bubbles. We explored the possibility to use several combined imaging sequences and use intensity differences between the super-paramagnetic labelled drug delivery system on the one hand and the susceptibility artefacts arising from other sources on the other hand.

The MRI contrast in organic tissue normally arises between regions showing different relaxation times (T_1 and T_2) depending on different relaxation mechanisms and/or different effectiveness of a relaxation process. This can be strengthened by materials containing paramagnetic or super-paramagnetic agents like iron oxide or Gd-chelates. Magnetite particles dephase the magnetization vector in their neighbourhood, which gives rise to a strong T_2^*-effect. In opposition to this, paramagnetic solutions of Gd-chelate mainly shorten the spin–lattice time T_1. Looking on liquids or tissues with non-fixed molecules (like almost all organic materials), the relaxation effects are often combined with MR-signal attenuation caused by diffusion [14,15].

MRI-susceptibility effects in a narrower sense arise in the neighbourhood of boundaries between volumes of different macroscopic magnetization. The macroscopic susceptibility effect can be quantified by its distortion effect (Δr) which depends directly on the magnetic field strength and the material susceptibility constant χ_m and inversely directly on the acquisition bandwidth. In the case of frequency encoding, the acquisition bandwidth should be proportional to the gradient strength of the read out gradient for matching the whole object [16].

However, the choice of a pulse sequence has a big influence on the susceptibility artefacts. For example, spin-echo sequences are known to be less sensitive compared to gradient echo sequences. The coherence between gradient and location is shifted by the additional local magnetic field, and the image shows some typical distortions (Fig. 1). In areas where the original linear gradient starts to be weakened by the (super-) paramagnetic particle, the spin density is diluted, and in areas where the influence of the particle decreases, the spin density increases. For a cylindrical shaped body, this leads to the typical arrow-like shape shown in Fig. 1 in a transversal section [11].

Using gradient echo sequences, the field inhomogeneities cause strong distortions and high signal loss in the areas influenced by susceptibility (Fig. 2). Gradient echoes are more influenced by diffusion in the local susceptibility field gradient. For example, in the case of slow diffusion, the magnetization is fully refocused by a spin-echo, but not for gradient echoes due to static line broadening. To sum it up, it can be said that gradient echo sequences are not only more sensitive to susceptibility effects, but also show another distortion pattern. The different behaviour of spin echoes and gradient echoes is an opportunity to increase the selectivity of the MRI contrasts between the drug delivery system and the surrounding food.

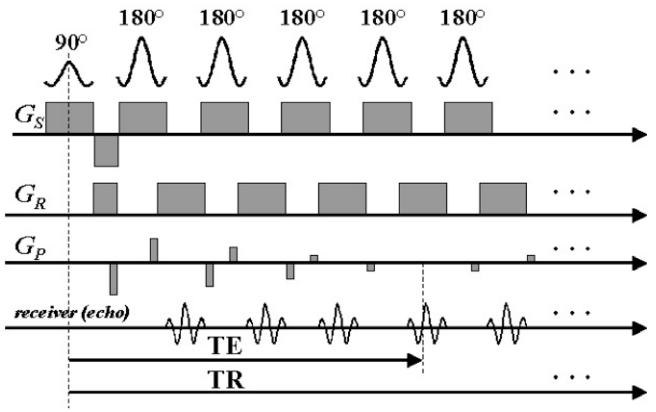

Fig. 2. *HASTE* sequence: *HASTE* (Half Acquisition Single Shot Turbo Spin Echo) is a very fast spin-echo sequence, which covers a little bit more than half of the *k*-space. The picture shows the rf-pulses, the time courses of the three gradients (slice, read, phase) and the echo formation of the first five *k*-space steps. Note that the echo time is defined as the time to the phase step of the center ($k = 0$) of *k*-space. Typical parameters are $TE \sim 100$ ms; $TR \sim 1000$ ms and >128 echoes after excitation which gives strong T_2-contrast.

2. Materials and methods

All ingredients were of pharmaceutical grade. Avicel PH101 came from FMC, lactose from Meggle and black iron oxide from BASF. Pellets were produced by a standard extrusion/spheronisation technology. They were composed of Microcrystalline cellulose (Avicel PH101) 70% (w/w), Lactose 29% (w/w) and Black Iron oxide (magnetite) 1% (w/w). The powder content was mixed in a cubic mixture for 10 min. In a second step, the mixed powders were granulated with water at a 1:1 (w/w) ratio in a kneader. Thereafter, the wet mass was extruded at 40 rpm in a radial screen twin-screw extruder (Fuji-Paudal, Japan) equipped with a die of 1 mm diameter circular openings and 1 mm thickness. The extrudate was then spheronised for 3 min in a 250 mm radial plate spheronizer (Fuji-Paudal, Japan), using a cross-hatch frictional plate of 3×3 mm^2 pitch and 1.2 mm depth. The resulting pellets were then dried in an oven at 50 °C until a constant weight has been reached. The resulting pellets for MRI measurements had a diameter of 1 mm.

The ingested food consisted of a yogurt (low fat yoghurt from Euco GmbH). For in vitro measurements, a 1:1 mixture of the yoghurt with curd cheese (Speisequark, Euco GmbH) was used to prevent sedimentation of the pellets during the measurement.

2.1. Sequences

MR examinations were performed on a 1.5 T scanner (MAGNETOM Sonata; Siemens Medical Systems, Erlangen, Germany) equipped with high performance gradients characterized by an amplitude of 40 mT/m and a slew rate of 200 mT/m/ms. The pulse sequences used for the detection of susceptibility artefacts in the stomach should have T_2-weighted soft tissue contrast and short acquisition time to prevent motion artefacts and for measuring the whole stomach in one breath hold cycle. However, they should have different sensitivity against susceptibility effects. For these reasons, *HASTE*-sequence and a *TRUFI* sequence were chosen. Both sequences need roughly 1 s per slice. The measurement time strongly depends on the number of slices thus make it possible to adjust the measurement time to the breath hold capability of the test person. The location of the measured slices was chosen identical for both sequences.

2.2. HASTE

HASTE (Half Acquisition Single Shot Turbo Spin Echo, Figs. 2 and 4) is a very fast variant of a turbo spin echo showing a high turbo factor and an acquisition of roughly half (<60%) of the *k*-space resulting in a measuring time of ~1 s per slice. The sequence gives a strong T_2 contrast due to a long effective echo time (TE^{eff}) and a long repetition time TR. Typically for a spin-echo sequence, the images are relatively free of motion and chemical shift artefacts, and as a main fact, they show only poor susceptibility artefacts (Fig. 4).

(Parameter settings: pulse sequence: -t2_haste_tra_bh; flip angle: $\alpha = 150°$; resolution: $1.17 * 1.17 * 6.5$ mm^3 $(256 * 256 * 14)$; $TE = 117$; $TR = 1000$.)

2.3. TRUFI

TRUFI (True FISP, True Fast Imaging with Steady Precession, Figs. 3 and 5) is a balanced steady-state free precession (bSSFP) sequence with a contrast in dependence of the ratio T_1/T_2 and the flip angle α. However, for the chosen parameters, the contrast is nearly T_2-weighted and stronger than that from the *HASTE*-sequence. A special feature of bSSFP sequences is an off-resonance artefact arising from breaking down the steady state magnetization for a dephasing angle of exact 180° (and a multitude) in relation to the transmitter frequency [17] (Scheffler et al., 2003). This gives

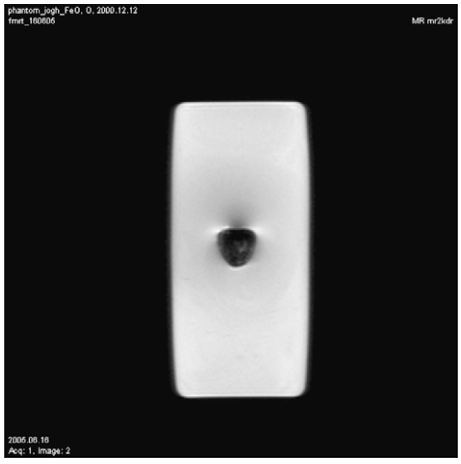

Fig. 4. Typical susceptibility artifacts of a T_2-weighted turbo spin-echo sequence. (*HASTE*-sequence: *TE* 140 ms, *TR* 3000 ms). The object is a glassy tube (Ø2.51 cm) containing 0.1% magnetite in a 5% hydroxyethylcellulose gel. The tube is surrounded by pure yogurt.

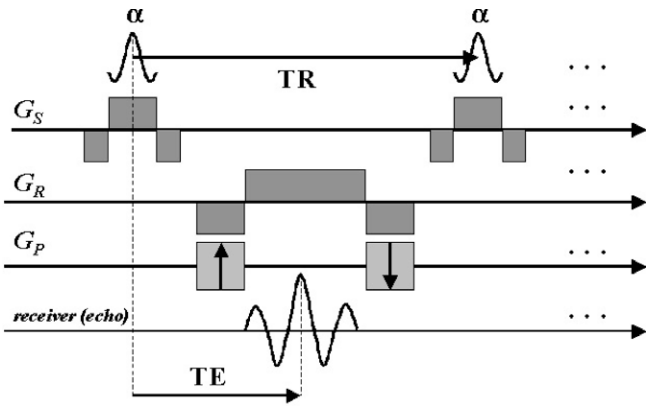

Fig. 3. *TRUFI* sequence: *TRUFI* (True *FISP*, True Fast Imaging with Steady Precession) is a balanced steady-state free precession (bSSFP) gradient echo sequence. After the first (~5) echoes, a steady state of the magnetization will be established which gives T_2/T_1-weighted image contrast. Typical parameters are $TE \sim 2$ ms; $TR \sim 4$ ms, >128 echoes and a flip angle $\alpha = 70–90°$.

Fig. 5. Typical susceptibility artifacts of a balanced steady-state free precession (bSSFP) sequence showing T_2/T_1-contrast. (*TRUFI*-sequence: *TE* = 2.15 ms, *TR* = 4.3 ms; $\alpha = 74°$.) For materials and experimental setup see Fig. 4.

an additional contrast in the region of macroscopic field inhomogeneities caused by strong susceptibility changes. These artefacts resemble thin dark magnetic field lines which extend far away from the surfaces/interfaces (Fig. 5).

(Parameter settings: pulse sequence: -t2_trufi_tra_bh; flip angle: $\alpha = 62°$; resolution: $1.17 * 1.17 * 6.5\ mm^3$ $(256 * 256 * 14)$; $TE = 1.81$; $TR = 3.62$.)

2.4. Methods of data acquisition and data processing

The basic idea for mapping a strongly susceptibility weighted image is the voxel-by-voxel comparison of the slices of both sequences. Only structures arising from effects, which strongly differ between the two image sets (e.g. susceptibility artefacts) will be emphasized by this procedure. The method involves the following steps:

- Taking up two geometric-identical volume data sets of the two modalities.
- Adjustment of the overall intensity level of the one modality to the other.
- Voxel-by-voxel subtraction of the *TRUFI* from the *HASTE* data set.
- Define an intensity threshold of the contrast. This should be done very carefully to select the real susceptibility from other contrast effects and noise.
- The resulting map can be superimposed on one of the two acquired series of images for the exact localization of susceptibility artefacts.

3. Results and discussion

3.1. In vitro results

To demonstrate the capability of the suggested method, it was tested in a 20 cm * 10 cm * 9 cm PE-box filled with a viscous milk product (pure yogurt) for simulation of a human stomach volume. Several distinct food pieces (bread, fruits, meat) were placed beside the magnetite (1%)-loaded pellets. The experimental in vitro setup guaranties – in opposite to a real stomach – a motion free measurement. The results are shown in Fig. 6. It can be stated that an unambiguous identification of small ferric oxide particles among other food items in slices of 8 mm is possible.

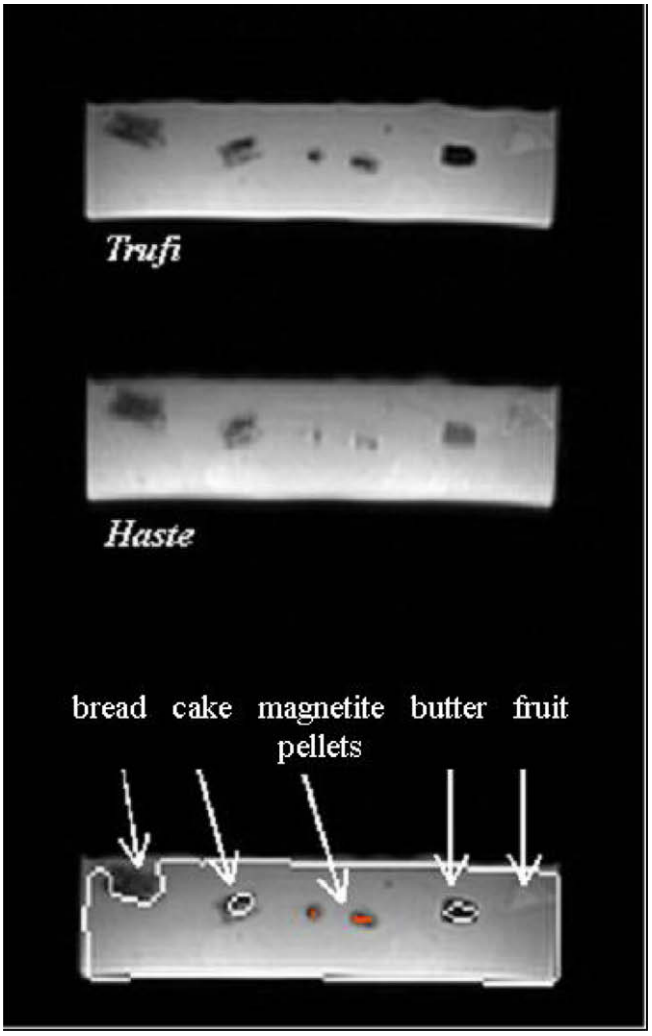

Fig. 6. In vitro measurement of different food items suspended in yogurt. Each figure shows the same slice (180 mm × 50 mm; thickness 8 mm) of the in vitro setup: top: *TRUFI*, middle: *HASTE*, bottom: susceptibility contrast calculated by the described procedure. Only the red-marked spots show susceptibility contrast. All other low intensity areas arise from non-susceptibility in homogeneities. Notice that the pellets (¢ 1 mm, see Fig. 1) can be observed in a slice of 8 mm due to the susceptibility artifacts. (For interpretation of color mentioned in this figure the reader is referred to the web version of the article.)

3.2. In vivo results

The major problem for the use of the method described earlier for investigations of the human gastrointestinal tract is the gastric motion itself. The grinding and emptying process of a meal takes several hours, but peristaltic waves show periods of 15–20 s at maximum velocities from 1.8 to 2.4 mm/s in the distal stomach [18,19]. To minimize motion effects, the measurements of both the modalities should be inside a breath hold cycle. So, the number of slices was reduced to 2 * 12 consecutive images of both modalities giving a measurement time of about 25 s. Using a slice thickness of 8 mm, this covers an area of 96 mm. For an investigation of the whole stomach including pylorus and duodenum, a repetition of the measurement with more distal coordinates can be necessary. However, the short period stomach motion complicates the comparison between the *TRUFI* and the *HASTE*-images. To overcome this, an additional co-registration of the two modalities was developed. For this, the Matlab (The MathWorks, Inc.)-based segmentation and co-registration tool of SPM (Statistical Parametric Mapping, The FIL methods group of the University College London) software were used. *HASTE* and *TRUFI* pilot images were recorded. The intensity ratio was determined from the averaged grey intensities. This ratio was used to modify the parameter settings for the following in vivo co-registration of both sequences. As a result, almost equally intensive *HASTE* and *TRUFI* images were obtained. The *TRUFI* image was subtracted from the *HASTE* image. As a result, mainly structures with large differences in susceptibility were obtained.

After the co-registration of the *HASTE* to the *TRUFI*-slices, the further steps are equal to the in vitro procedure (voxel subtraction, determination of the susceptibility threshold, superimposition of the susceptibility map to an anatomical picture). The choice of a right threshold which separates the susceptibility artefacts from other artefacts is the critical point of the method. However, good results were obtained with thresholds taken from the in vitro experiments. Two examples of in vivo measurements are shown in the Figs. 7 and 8. Volunteer #1 (Fig. 7) took a special meal with 200 g poor yogurt and 100 ml table water giving high intensity in T_2-weighted contrast. Some bits of additional food (bread, banana, meat) gave additional contrast. All seven magnetite-labelled pellets could be detected without difficulty. In a more challenging

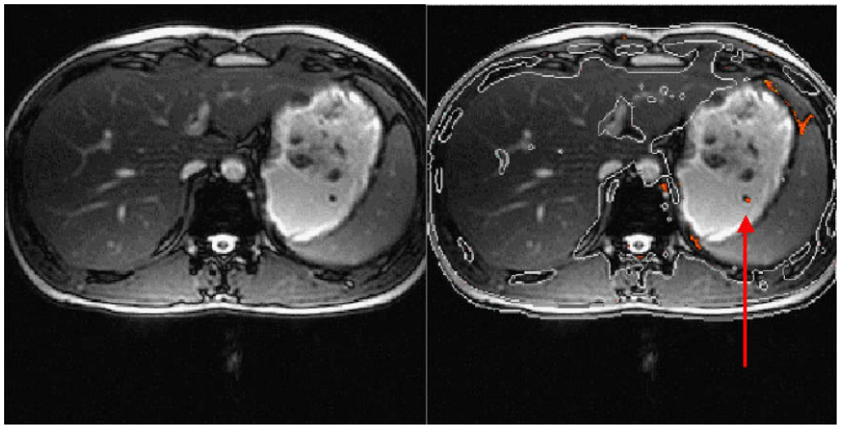

Fig. 7. Left: anatomical image (*TRUFI*, 8 mm slice) of the abdomen (transversal slice) of a volunteer (#1) eating a heterogeneous meal (200 g yogurt with some bred, cake, banana) and seven magnetite pellets. Right: only the magnetite-marked pellet is set off by the red-colored susceptibility map (arrow). Marked areas outside the stomach volume come from motion artifacts. The other pellets were found in a similar manner in other layers. (For interpretation of color mentioned in this figure the reader is referred to the web version of the article.)

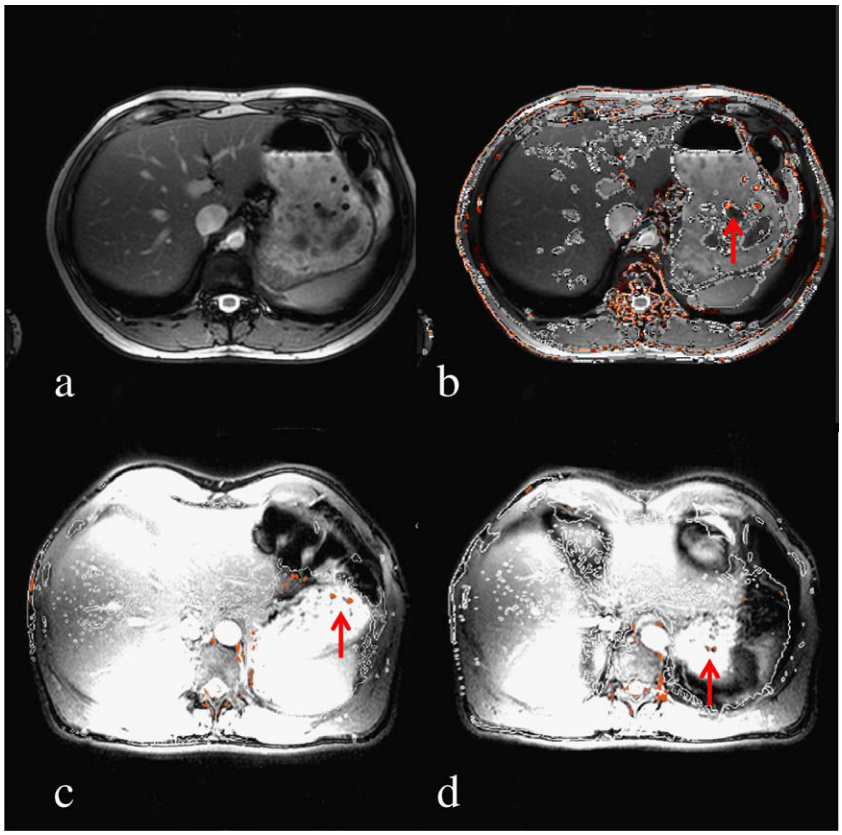

Fig. 8. (a) Anatomical image (*TRUFI*, 8 mm slice) of the abdomen of a volunteer (#2) eating a heterogeneous "standard" meal (potatoes, vegetable, meat). Some of the magnetite pellets are seen already as low signal areas. (b) Magnetite pellets are set off by the susceptibility map (four are seen near the arrow) co-registered to the anatomical image (*TRUFI*). Marked areas outside the stomach volume arising from motion artifacts and strong susceptibility artifacts of the vertebra. (c and d) Susceptibility marked slices processed like (b) from two different slices (6 mm) of the abdomen of volunteer (#3). Among some artifacts outside the stomach, a couple of pellets can be seen in each slice. (For interpretation of color mentioned in this figure the reader is referred to the web version of the article.)

and realistic setup (volunteer #2 and #3), the "standard" meal consisted of meat, potatoes and some vegetable, cake, and a soft drink (<100 ml). As expected, the MRI contrast differences between the some food components and the pellets were much lower compared to the first case. Especially, food with a high content of fat showed nearly the same contrast as the magnetite-labelled pellets did (see also Fig. 6). However, with a careful optimization of the new imaging procedure, an adjustment of the susceptibility threshold a differentiation was possible. Unfortunately, a standard fitting of the susceptibility threshold works until now only for the in vitro experiments but not for the in vivo experiments. The threshold varies between both volunteers and slices. Normally, one gets an acceptable result starting by a low value and then rises it step by step until the suspect structures show first contrast. Also, the

suppression of susceptibility artefacts outside the stomach (e.g. surface of bones, vertebra) was generally not possible.

In addition, the stomach contractions of the second volunteer were stronger and faster while the measurement duration of ~24 s could be seen by a direct comparison of both series of images. Not in all cases, the co-registration procedure was able to superpose the two series perfectly. Therefore, some of the red-labelled artefacts (Fig. 8) may arise from imperfect superposition. Despite these problems, an identification of all 7 pellets was possible again even in this complex and highly heterogeneous environment.

4. Conclusions

With this developed method, it is feasible to monitor individual pellets or other small multi-particulates in the human stomach. The MRI detection of multi-particulates in vivo is very challenging, due to the small size of multi-particulates, their low MRI contrast and the complex MRI features of food (including low and high signal intensities and air bubbles). This makes the MRI detection of unlabelled multi-particulates by MRI impossible. The prerequisite (and therefore also a limitation) for our method is the incorporation of magnetite, which causes MRI artefacts. However, the necessary load is rather low. In the current study, a load of 1% (w/w) was used. The magnetite (=black iron oxide) gives a low signal intensity and therefore a bright contrast to high signal intensity food items (e.g. fat, food with water). However, low MRI signal intensities also arise from unhydrated, solid food or entrapped air. Compared to tablets and capsules, the small size of the multi-particulates makes a differentiation between the drug delivery system and the environment much more difficult. A method was therefore developed to differentiate between the contrast coming from susceptibility effects (caused by the magnetite-loaded pellet) and the low intensity areas due to other objects (mainly more solid like residuals of the food and air bubbles) of a heterogeneous meal. A challenge is the influence of gastric motion. Future work will be done to develop more appropriate sequence with a fast cycling of the two pulse sequences. This could improve the time-resolution to nearly two seconds, what should be enough for the elimination of gastric motion artefacts. In comparison with methods which use only one MRI sequence modality (e.g. T_1- or T_2-weighted gradient echo sequences), the sensitivity and selectivity of this subtraction method is very high. As a result, the amount of magnetite could be reduced in strength (e.g. 0.1% Fe_3O_4) or even smaller particles might be detected. Future work will be dedicated to establish procedures for the automatic processing of the MRI images and the extraction of the data.

In summary, the new method greatly extends the application of MRI to follow the fate of multi-particulate oral drug delivery systems in humans. Future studies will also explore the possibility to follow multi-particulates in the small and large intestine.

References

[1] J. Timmermans, A.J. Moës, The cutoff size for gastric emptying of dosage forms, J. Pharm. Sci. 82 (1993) 854.
[2] K. Higaki, S.Y. Choe, R. Löbenberg, L.S. Welage, G.L. Amidon, Mechanistic understanding of time-dependent oral absorption based on gastric motor activity in humans, Eur. J. Pharm. Biopharm. 70 (2008) 313–325.
[3] S.S. Davis, J.G. Hardy, S.P. Newman, I.R. Wilding, Gamma scintigraphy in the evaluation of pharmaceutical dosage forms, Eur. J. Nucl. Med. 19 (1992) 971–986.
[4] I.R. Wilding, D.V. Prior, Remote controlled capsules in human drug absorption (HDA) Studies, Crit. Rev. Ther. Drug. 20 (2003) 405–431.
[5] J.C. Richardson, R.W. Bowtell, K. Mäder, C.D. Melia, Pharmaceutical applications of magnetic resonance imaging (MRI), Adv. Drug Deliv. Rev. 57 (2005) 1191–1209.
[6] W. Weitschies, O. Kosch, H. Mönnikes, L. Trahms, Magnetic marker monitoring: an application of biomagnetic measurement instrumentation and principles for the determination of the gastrointestinal behavior of magnetically marked solid dosage forms, Adv. Drug Deliv. Rev. 57 (2005) 1210–1222.
[7] W. Weitschies, Magnete statt Radioisotope: Pillen auf der Spur, Pham. unserer Zeit. 29 (2000) 15–120.
[8] L.A. Cora, F.G. Romeiro, M. Stelzer, M.F. Americo, R.B. Oliveira, O. Baffa, J.R.A. Miranda, AC biosusceptometry in the study of drug delivery, Adv. Drug Deliv. Rev. 57 (2005) 223–1241.
[9] D.J. Lurie, Proton–electron double-resonance imaging (PEDRI), in: L.J. Berliner (Ed.), In Vivo EPR (ESR) – Biological Magnetic Resonance, vol. 18, Kluwer Academic/Plenum Publishers, New York, USA, 2003, pp. 547–578.
[10] D.J. Lurie, K. Mäder, Monitoring drug delivery processes by EPR and related techniques – principles and applications, Adv. Drug Deliv. Rev. 57 (2005) 1171–1190.
[11] D. Bilecen, K. Scheffler, E. Seifritz, G. Bongartz, W. Steinbrich, Hydro-MRI for the visualization of gastric wall motility using RARE magnetic resonance imaging sequences, Abdom. Imaging 25 (2000) 30–34.
[12] A. Steingoetter, D. Weishaupt, P. Kunz, K. Mäder, H. Lengsfeld, M. Thumshirn, P. Boesiger, M. Fried, W. Schwizer, Magnetic resonance imaging for the in vivo evaluation of gastric-retentive tablets, Pharm. Res. 20 (2003) 2001–2007.
[13] A. Steingötter, P. Kunz, D. Weishaupt, K. Mäder, H. Lengsfeld, M. Thumshirn, P. Boesiger, M. Fried, W. Schwizer, Analysis of the meal-dependent intragastric performance of a gastric-retentive tablet assessed by magnetic resonance imaging, Aliment Pharmacol. Therap. 18 (2003) 713–720.
[14] S. Posse, W.P. Aue, Susceptibility artifacts in spin-echo and gradient-echo imaging, J. Magn. Reson. 88 (1990) 473–492.
[15] P.T. Callaghan, L.C. Forde, C.J. Rofe, Correlated susceptibility and diffusion effects in NMR microscopy using both phase-frequency and phase-phase encoding, J. Magn. Reson. A 104 (1994) 34–52.
[16] H. Fischer, R. Ladebeck, Echo-planar imaging image artifacts, in: F. Schmitt, M.K. Stehling, R. Turner (Eds.), Echo-Planar Imaging: Theory, Technique and Application, Springer, 1998.
[17] K. Scheffler, S. Lehnhardt, Principles and application of balanced SSFP techniques, Eur. Radiol. 13 (2003) 2409–2418.
[18] W. Ajaj, S.C. Goehde, N. Papanikolaou, G. Holtmann, S. Ruehm, J.F. Debatin, T.C. Lauenstein, Real time high resolution magnetic resonance imaging for the assessment of gastric motility disorders, Gut 53 (2004) 1256–1261.
[19] K. Indireshkumar, J.G. Brasseur, H. Faas, G.S. Hebbard, P. Kunz, J. Dent, C. Feinle, M. Li, P. Bösiger, M. Fried, W. Schwizer, Relative contributions of "pressure pump" and "peristaltic pump" to gastric emptying, Am. J. Physiol. Gastrointest. Liver Physiol. 278 (2000) G604–G616.